FREQUENCY STANDARDS, CHARACTERIZATION

In this article we describe the characterization of frequency standards following the general definitions accepted by the IEEE, the International Telecommunication Union-Radiocommunications (ITU-R), and International Radio Consultative Committee (CCIR) (1–3). In using the term "frequency standard" we imply that changes in the frequency $\Delta\nu$ of the device are small compared to its nominal frequency ν_0 and that therefore the frequency would be about the same if we were to remeasure it. This permits us to treat the variations in fractional frequency $\Delta\nu/\nu_0$ as small compared to 1, and this greatly simplifies the mathematics of the characterization. We describe what is meant by accuracy and frequency stability of a frequency standard. The variations in frequency (which define the frequency stability) can be classified into two basic types, random and systematic. To characterize the random variations in frequency the systematic effects must be removed from the data. Special statistical techniques other than the standard variance must then be used to quantify the random variations in frequency, because some of the noise processes are not stationary. By this we mean that the mean of the frequency noise changes slowly with time. As part of the statistical treatment we describe how to determine the confidence intervals for the estimates of the various types of random frequency noise.

ACCURACY

Frequency standards generate a periodic voltage signal, whose ideal frequency is defined as a specific number of oscillations per second. The second is the agreed unit of time, based on the energy difference between two energy levels of the unperturbed cesium atom (4), and it is this definition that allows the specification of accuracy of a frequency standard. Generally there will be offsets or biases in the actual frequency of a standard when compared to the ideal or defined value (according to the definition of the second) due to systematic and random effects (5–7). The *accuracy* of a frequency standard, more recently described as an uncertainty, is a

measure of the confidence relative to a physical model of the standard and the evaluation process. To evaluate the accuracy of a frequency standard, a list of known sources of frequency offsets is made, and the offset or bias due to each source and its uncertainty are carefully measured or computed. The uncertainty is a proper summation of the estimates of various systematic offsets and random noise (8). For example, a frequency standard with an output frequency of 10 MHz and an uncertainty of 10^{-8} has an frequency error of $\leq \pm$ 0.1 Hz.

STABILITY

Figure 1 shows the output voltage signal of an ideal *frequency standard* as a function of time. The maximum value V_0 is the nominal amplitude of the signal. The time required for the signal to repeat itself is the period T of the signal. The nominal frequency ν_0 of the signal is the reciprocal of the period, $1/T$. This voltage signal can be represented mathematically by a sine function,

$$v(t) = V_0 \sin\theta = V_0 \sin(2\pi\nu_0 t) \tag{1}$$

where the argument $\theta = 2\pi\nu_0 t$ of the sine function is the nominal phase of the signal. The time derivative of the phase θ is $2\pi\nu_0$ and is called the nominal angular frequency ω_0. In the frequency domain, this ideal signal is represented by a delta function located at the frequency of oscillation. Since this signal is ideal, there are no known sources that cause frequency shifts, and thus its frequency is *totally* accurate and its uncertainty is 0. Furthermore, its frequency, phase, and amplitude are constant; therefore the signal is also stable in frequency, phase, and amplitude.

In real situations, the output signal of an oscillator (source) or frequency standard has noise. Such a *noisy signal* is illustrated in Fig. 2. In this example we have depicted a case where the noise power is much less than the signal power. Frequency instability is the result of fluctuations in the period of the signal. Amplitude instability is the result of fluctuations in the peak values of the voltage. Phase instability is the result of fluctuations in the zero crossings. Since the period (and thus the frequency) of the signal is related to its phase, frequency instability and phase instability are directly related.

Figure 3 shows the *power spectrum of a noisy signal* (power as a function of frequency) as measured by a spectrum analyzer. Although the maximum power occurs at the frequency of oscillation, other peaks are observed at frequencies of $2\nu_0$, $3\nu_0$, . . ., $n\nu_0$, where n is a positive integer. These frequencies are called *harmonics* of the fundamental frequency ν_0; $2\nu_0$ is the second harmonic, $3\nu_0$ is the third harmonic, and so on. The power at these harmonic frequencies will depend on the design of the source. The spectrum around the fundamental frequency displays power sidebands at frequencies above the carrier (upper sideband) and at frequencies below the carrier (lower sideband). These power sidebands are the result of phase fluctuations and amplitude fluctuations in the signal. While the power spectrum gives an idea of the total noise of a signal, it does not give information about the relative magnitude of its phase instabilities and amplitude instabilities. Furthermore, at frequencies close to ν_0 it is difficult to separate the noise power from the power of the fundamental frequency. Therefore, special measurement techniques are needed to measure phase instabilities and amplitude instabilities in sources.

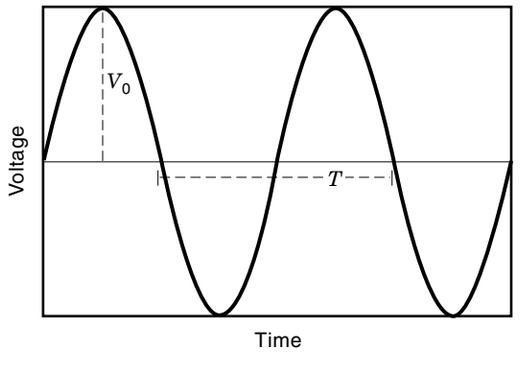

Figure 1. Ideal output voltage of a frequency standard.

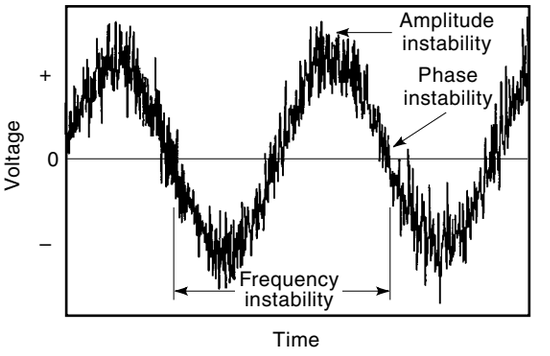

Figure 2. Output voltage of a noisy signal.

A *noisy signal* can be mathematically represented by

$$v(t) = [V_0 + \epsilon(t)] \sin[2\pi\nu_0 t + \phi(t)] \tag{2}$$

where $\epsilon(t)$ represents amplitude fluctuations (amplitude deviation from the nominal amplitude V_0) and $\phi(t)$ represents phase fluctuations (phase deviation from the nominal phase $2\pi\nu_0 t$) (1). The instantaneous frequency of this signal is defined as

$$\nu(t) = \frac{1}{2\pi}\frac{d}{dt}(\text{phase}) = \nu_0 + \frac{1}{2\pi}\frac{d}{dt}\phi(t) \tag{3}$$

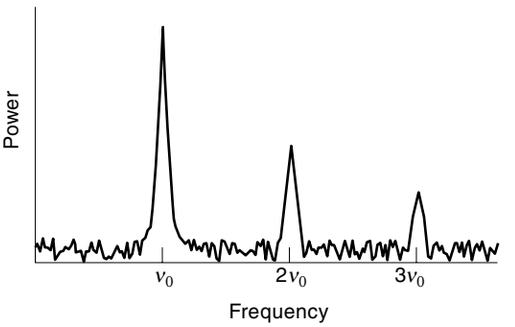

Figure 3. Power spectrum of a noisy signal.

Frequency fluctuations refer to the deviation $\nu(t) - \nu_0$ of the instantaneous frequency from the nominal frequency. Fractional frequency fluctuations, denoted as $y(t)$, refer to frequency fluctuations normalized to ν_0; that is,

$$y(t) = \frac{\nu(t) - \nu_0}{\nu_0} = \frac{1}{2\pi\nu_0}\frac{d}{dt}\phi(t) \tag{4}$$

Equation (4) indicates that there is a direct relation between phase fluctuations and fractional frequency fluctuations. Therefore, if a signal exhibits a certain amount of phase fluctuation, it also exhibits frequency fluctuation given by Eq. (4). The *time deviation* $x(t)$ of a signal is the integral of $y(t)$ from 0 to t. Thus one can write

$$y(t) = \frac{d}{dt}x(t) \tag{5}$$

The frequency stability of a frequency standard is affected by random noise processes and by systematic, deterministic changes. Systematic effects often dominate the frequency stability in nonlaboratory environments. The sensitivity of the standard to temperature, humidity, atmospheric pressure, magnetic field, and radiation may play a role (9–11). Generally, frequency (and thus phase) stability is divided into three regions: short-term, medium-term, and long-term stability. (Though the term frequency stability is used throughout most of the literature, the term actually refers to instabilities in the frequency.)

Short-term frequency stability refers to the random, nonsystematic fluctuations that are related to the signal-to-noise ratio of the device. In quartz crystal resonators this refers to the region dominated by white phase noise, where the time between observed frequencies (sample time) is less than a second. In atomic frequency standards the short-term stability also includes white frequency noise and extends to sampling times of several minutes.

Medium-term frequency stability refers to the region where flicker noise dominates. The sampling time characteristic of this region is a function of the type of frequency standard. Short-term and medium-term frequency stability can be characterized either in the frequency domain or in the time domain, after known systematic effects have been removed. Frequency-domain characterization and measurements are generally used when the sample time of interest is less than a second. For sampling times longer than a second, time-domain measurements are used to characterize frequency stability.

Long-term frequency stability includes random-walk frequency-noise processes in addition to systematic, deterministic changes in frequency observed when the sampling time is long. The long-term, systematic frequency change is called *frequency drift* (2,12). Drift includes frequency changes due to changes in the components of the source in addition to those due to external parameters such as temperature, humidity, pressure, magnetic field, and radiation (9–11). Frequency *aging,* on the other hand, refers to the long-term systematic frequency change due to changes in the components of the source, independent of parameters external to the source (2,12).

Frequency-Domain Characterization

Phase fluctuations in the frequency domain, or *phase modulation* (PM) *noise,* are characterized by the power spectral density (PSD) of the phase fluctuations, given by (13)

$$S_\phi(f) = \mathcal{F}[\mathcal{R}_\phi(\tau)] = \int_{-\infty}^{\infty} \mathcal{R}_\phi(\tau)e^{-j\omega\tau}\,d\tau \tag{6}$$

where $\mathcal{F}[\ ]$ is the Fourier transformation and $\mathcal{R}_\phi(\tau)$ is the autocorrelation function of the phase fluctuations given by

$$\mathcal{R}_\phi(\tau) = \langle\phi(\tau)\phi(t-\tau)\rangle \tag{7}$$

A more practical definition of PSD[$\phi(t)$] is

$$S_\phi(f) = \mathrm{PSD}[\phi(t)] = [\phi(f)]^2\frac{1}{\mathrm{BW}} \tag{8}$$

where $[\phi(f)]^2$ is the mean squared phase deviation at an offset frequency f from the frequency ν_0 (called the carrier in this context), and BW is the bandwidth of the measurement system (1,13–15). The offset frequency f is also called the Fourier frequency. The units for $S_\phi(f)$ are rad^2/Hz. Equation (8) is defined for $0 < f < \infty$; nevertheless it includes fluctuations from the upper and lower sidebands and thus is a double-sideband measure.

The PM noise measure recommended by the IEEE (1,14,15) is $\mathcal{L}(f)$, defined as

$$\mathcal{L}(f) \equiv \frac{S_\phi(f)}{2} \tag{9}$$

At Fourier frequencies far from the carrier frequency, where the integrated PM noise from ∞ to f (the Fourier frequency) is less than 0.1 rad^2, $\mathcal{L}(f)$ is equal to the single-sideband phase noise. The units for $\mathcal{L}(f)$ are decibels below the carrier in a 1 Hz bandwidth (dBc/Hz).

Frequency fluctuations in the frequency domain, or *frequency modulation* (FM) *noise,* are characterized by the power spectral density of the fractional frequency fluctuations, given by

$$S_y(f) = \mathrm{PSD}[y(t)] = [y(f)]^2\frac{1}{\mathrm{BW}} \tag{10}$$

where $y(f)^2$ represents the mean squared fractional frequency deviation at an offset (Fourier) frequency f from the carrier (1,13–15). $S_y(f)$ is defined for Fourier frequencies $0 < f < \infty$, and its units are inverse hertz.

The conversion between $S_y(f)$ and $S_\phi(f)$ can be obtained from Eq. (4). Applying the Fourier transformation to both sides of Eq. (4), squaring, and dividing by the measurement bandwidth results in

$$S_y(f) = \left(\frac{1}{2\pi\nu_0}\right)^2(2\pi f)^2 S_\phi(f) = \left(\frac{f}{\nu_0}\right)^2 S\phi(f) \tag{11}$$

Amplitude fluctuations in the frequency domain, or *amplitude modulation* (AM) *noise,* are characterized by the power

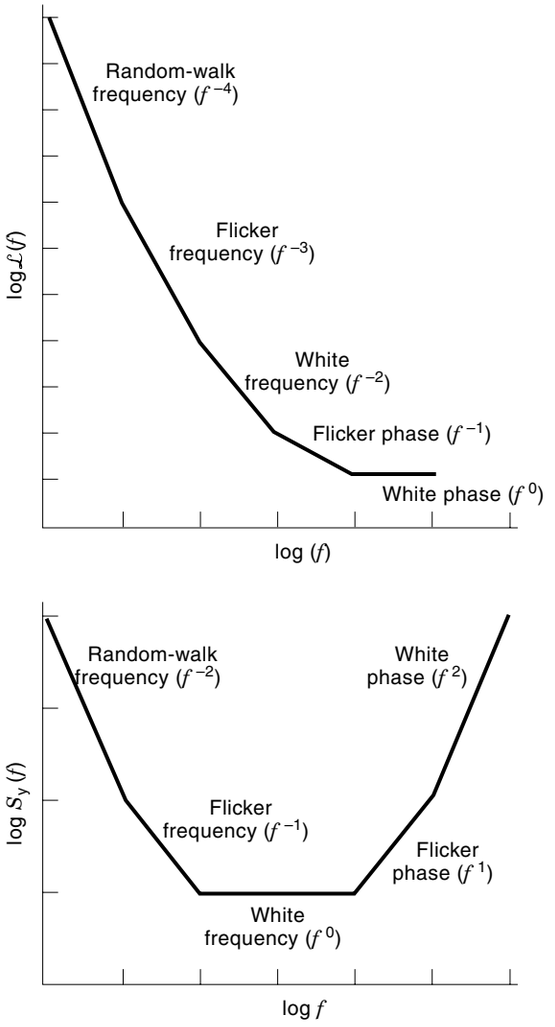

Figure 4. PM and FM noise characteristics of a source.

spectral density of the fractional amplitude fluctuations, given by

$$S_{\mathrm{a}}(f) = \mathrm{PSD}\left[\frac{\epsilon(t)}{V_0}\right] = \left(\frac{\epsilon(f)}{V_0}\right)^2 \frac{1}{\mathrm{BW}} \tag{12}$$

where $\epsilon(f)^2$ represents the mean squared amplitude deviation at an offset frequency f from the carrier (1). $S_{\mathrm{a}}(f)$ is defined for Fourier frequencies $0 < f < \infty$, and its units are inverse hertz.

In free-running sources, the FM noise is usually modeled by the sum of five different power laws or noise types as

$$S_{\mathrm{y}}(f) = \sum_{\alpha=-2}^{2} h_\alpha f^\alpha = h_{-2}f^{-2} + h_{-1}f^{-1} + h_0 f^0 + h_1 f^1 + h_2 f^2 \tag{13}$$

where $h_{-2}f^{-2}$ represents random-walk frequency noise, $h_{-1}f^{-1}$ represents flicker frequency noise, $h_0 f^0$ represents white frequency noise, $h_1 f^1$ represents flicker phase noise, and $h_2 f^2$ represents white phase noise. Similarly, the PM noise can be modeled by

$$S_\phi(f) = \sum_{\beta=-4}^{0} k_\beta f^\beta = k_{-4}f^{-4} + k_{-3}f^{-3} + k_{-2}f^{-2} + k_{-1}f^{-1} + k_0 f^0 \tag{14}$$

where $k_{-4}f^{-4}$ represents the random-walk frequency noise, $k_{-3}f^{-3}$ represents flicker frequency noise, $k_{-2}f^{-2}$ represents white frequency noise, $k_{-1}f^{-1}$ represents flicker phase noise, and $k_0 f^0$ represents white phase noise. Notice that $S_\phi(f)$ and $S_y(f)$ have different slopes for a specific type of noise, as implied by Eq. (11). Equation (11) can be used to obtain the conversion between the $S_\phi(f)$ and $S_y(f)$ coefficients, yielding

$$k_\beta = \nu_o^2 h_\alpha \qquad \text{for} \quad \beta = \alpha - 2 \tag{15}$$

Figure 4 shows the common noise types characteristic of the PM noise and the FM noise of a source (1,14–17). Usually a source exhibits two or three of the noise types shown in the plots (17).

The AM noise of a source can typically be modeled by the sum of three different power laws or noise types:

$$S_{\mathrm{a}}(f) = \sum_{\alpha=-2}^{0} h_\alpha f^\alpha = h_{-2}f^{-2} + h_{-1}f^{-1} + h_0 f^0 \tag{16}$$

where $h_{-2}f^{-2}$ represents random-walk amplitude noise, $h_{-1}f^{-1}$ represents flicker noise, and $h_0 f^0$ represents white amplitude noise (18). Figure 5 shows the common noise types characteristic of the AM noise of a source.

Upper and lower PM sidebands are always equal and 100% correlated. Likewise the upper and lower AM sidebands are always equal and 100% correlated. This is true even when the RF spectrum is not symmetric about the carrier (18a). The phase between AM and PM noise varies randomly with time for broadband additive noise (18a).

Time-Domain Characterization

In the time domain, the *fractional frequency stability* of a signal is usually characterized by the Allan variance, a type of two-sample frequency variance given by (1,13–15)

$$\sigma_{\mathrm{y}}^2(\tau) = \tfrac{1}{2}\langle(\overline{y}_{i+1} - \overline{y}_i)\rangle \tag{17}$$

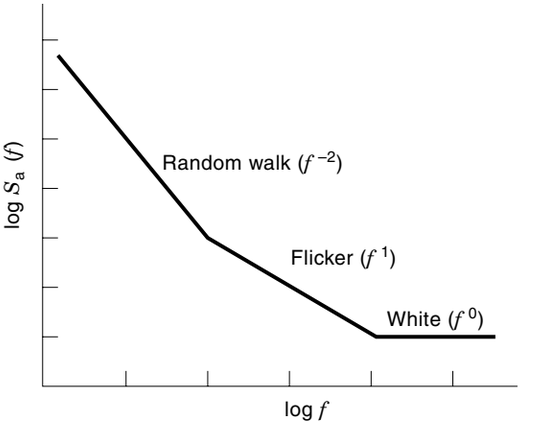

Figure 5. AM noise characteristics of a source.

where $\bar{y}_i$ is the average fractional frequency of interval i given by

$$\bar{y}_i = \frac{1}{\tau}\int_{t_i}^{t_{i+\tau}} y(t)\,dt = \frac{1}{\tau}[x(t_i+\tau) - x(t_i)] = \frac{1}{\tau}(x_{i+1} - x_i) \quad (18)$$

In practical situations only a finite number of fractional frequency samples are available, and the Allan variance is approximated by

$$\sigma_y^2(\tau) \approx \frac{1}{2(M-1)}\sum_{i=1}^{M-1}(\bar{y}_{i+1} - \bar{y}_i)^2 \quad (19)$$

where $M = N - 1$ is the number of frequency samples (N is the number of time samples) (1,14,15). The Allan variance can also be expressed in terms of time samples using $\bar{y}_i = (x_{i+1} - x_i)/\tau$:

$$\sigma_y^2(\tau) \approx \frac{1}{2(N-2)\tau^2}\sum_{i=1}^{N-2}(x_{i+2} - 2x_{i+1} + x_i)^2 \quad (20)$$

The square root of the Allan variance is called the Allan deviation, $\sigma_y(\tau)$.

When time samples are taken every τ_0 seconds, the Allan variance can be computed for several sampling times $\tau = n\tau_0$ where $n > 0$. For $n > 1$, overlapped samples can be used to compute σ_y^2 as shown in Fig. 6, providing better confidence intervals (1,19). An expression for the fully overlapped Allan variance can be derived using Fig. 6 and Eq. (19). For $\tau = n\tau_0$ Eq. (19) becomes

$$\sigma_y^2(\tau) \approx \frac{1}{2(M-2n)}\sum_{i=1}^{M-2n}(\bar{y}_{i+n} - \bar{y}_i)^2 \quad (21)$$

which can also be expressed in terms of time-domain data by substituting $\bar{y}_i$ for $(x_{i+n} - x_i)/n\tau_0$:

$$\sigma_y^2(\tau) \approx \frac{1}{2(N-2n)\tau^2}\sum_{i=1}^{N-2n}(x_{i+2n} - 2x_{i+n} + x_i)^2 \quad (22)$$

Figure 7(a) shows a log–log plot of the Allan variance as a function of the sampling time τ for a source that exhibits all five common noise types. The slopes of the white PM noise and the flicker PM noise are the same; therefore these two noise types cannot be separated using this plot. The Allan variance can often be modeled by the sum of four different power laws:

$$\sigma_y^2(\tau) = \sum_{\mu=-2}^{1} p_\mu \tau^\mu = p_{-2}\tau^{-2} + p_{-1}\tau^{-1} + p_0\tau^0 + p_1\tau^1 \quad (23)$$

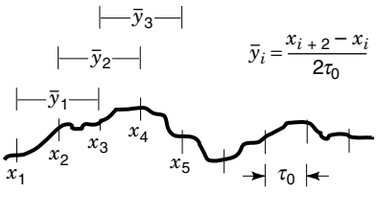

Figure 6. Computation of $\{\bar{y}_i\}$ for the overlapped Allan variance and $n = 2$.

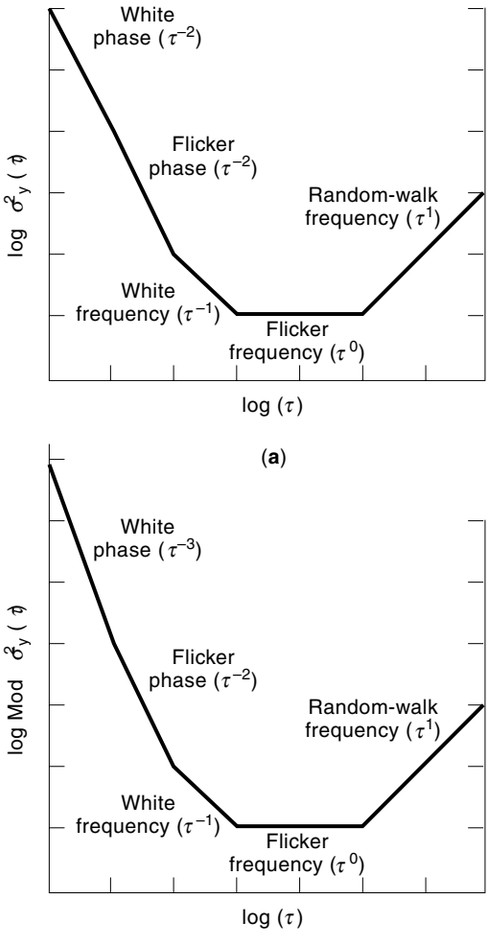

Figure 7. $\sigma_y^2(\tau)$ and Mod $\sigma_y^2(\tau)$ for the five noise types.

where $p_{-2}\tau^{-2}$ represents white phase and flicker phase noise, $p_{-1}\tau^{-1}$ represents white frequency noise, $p_0\tau^0$ represents flicker frequency noise, and $p_1\tau^1$ represents random walk frequency noise.

When the dominant noise type in the short term is flicker PM or white PM, the modified Allan variance can be used to improve the estimate of the underlying frequency stability of the sources (1,14,20). Here a new series $\{\bar{x}_i\}$ is created by averaging n adjacent phase (time) measurements of duration τ_0. The average fractional frequencies are computed from the $\{\bar{x}_i\}$, as illustrated in Fig. 8. For N time samples and $\tau = n\tau_0$, the resulting modified Allan variance is

$$\text{Mod}\,\sigma_y^2(\tau) \approx \frac{1}{2(N-3n+1)}\sum_{i=1}^{N-3n+1}(\bar{y}'_{i+n} - \bar{y}'_i)^2 \quad (24)$$

Equation (24) can also be expressed in terms of the initial time-domain data $\{x_k\}$:

$$\text{Mod}\,\sigma_y^2(\tau) \approx \frac{1}{2\tau^2 n^2(N-3n+1)}\sum_{j=1}^{N-3n+1}\left[\sum_{i=j}^{n+j-1}(x_{i+2n} - 2x_{i+n} + x_i)\right]^2 \quad (25)$$

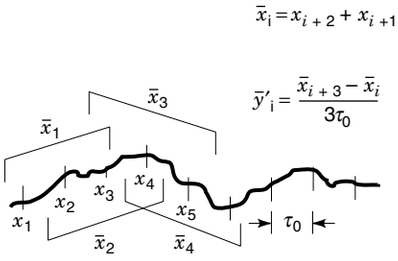

Figure 8. Computation of $\{\bar{x}_i\}$ and $\{\bar{y}_i\}$ for the Modified Allan variance and n = 3.

where

$$\bar{y}'_i = \frac{\bar{x}_{i+n} - \bar{x}_i}{\tau} \tag{26}$$

and

$$\bar{x}_i = \frac{\sum_{k=0}^{n-1} x_{i+k}}{n} \tag{27}$$

Here $\bar{x}_i$ is the phase (time) averaged over n adjacent measurements of duration τ_0. Thus Mod $\sigma_y(\tau)$ is proportional to the second difference of the phase averaged over a time $n\tau_0$. Viewed from the frequency domain, Mod $\sigma_y(\tau)$ is proportional to the first difference of the frequency averaged over n adjacent samples. The square root of the modified Allan variance is called the modified Allan deviation Mod $\sigma_y(\tau)$.

Figure 9 shows the ratio $R(n) = [\text{Mod } \sigma_y^2(\tau)]/\sigma_y^2(\tau)$ as a function of n for all five types of noise processes (15). For random-walk FM, flicker FM, and white FM the ratio is constant for $n \geq 5$. Therefore, Mod $\sigma_y^2(\tau)$ and $\sigma_y^2(\tau)$ have the same slope for these noise types. For white PM noise ($\alpha = 2$), the slope is $-1/n$; therefore the slope of Mod $\sigma_y^2(\tau)$ is equal to the slope of $\sigma_y^2(\tau)$ divided by τ. Finally, for flicker PM noise the ratio asymptotically reaches $3.37/(1.04 + 3 \ln \omega_h\tau$. In this case and for $n > 10$, the slope of Mod $\sigma_y^2(\tau)$ is approximately τ^{-1}. Figure 9 also shows that Mod $\sigma_y^2(\tau)$ is considerably smaller than $\sigma_y^2(\tau)$ for white PM and flicker PM noise. Not only does Mod $\sigma_y^2(\tau)$ provide a different slope for white PM noise and flicker PM noise, allowing the separation of the two noise processes (see Fig. 7b); it can also speed the stability measurements. If a system is limited by white and flicker PM noise at short average times, using Mod $\sigma_y^2(\tau)$ reduces the measurement time required to observe white FM, flicker FM, and random-walk FM at longer averaging times, in comparison with that required when using $\sigma_y^2(\tau)$ (15).

At long averaging times when the ratio $N\tau_0/(2n\tau_0)$ is close to 1, the Allan variance has a bias related to its insensitivity to odd noise processes in the phase (time) fluctuations (odd with respect to the midpoint). In these situations an extension of the Allan variance that removes this bias can be used to characterize the frequency stability of a source. This variance, $\sigma_{y,\text{TOTAL}}^2(\tau)$, is obtained by extending the $\{x_i\}$ in both directions and then computing the Allan variance from the new $\{x_i'\}$ sequence (21–23). Figure 10 illustrates this extension of $\{x_i\}$: on the left side the extension is the inverted mirror image of $\{x_i\}$ with respect to x_1; on the right side it is the inverted mirror image of $\{x_i\}$ with respect to x_N. How far this extension depends on the maximum value n_m of n. For N time data points, n_m is the integer part of $(N - 1)/2$. The far-left data point is $x'_{2-n_m} = 2x_1 - x_{n_m}$; the far-right data point is $x'_{N+n_m-1} = 2x_N - x_{N-n_m+1}$. Thus $\sigma_{y,\text{TOTAL}}^2(\tau)$ is given by

$$\hat{\sigma}_{y,\text{TOTAL}}^2(\tau) = \frac{1}{2(N-2)} \sum_{i=2}^{N-1} (\bar{y}'_i - \bar{y}'_{i-n})^2 \tag{28}$$

Equation (28) can be expressed in terms of $\{x_i'\}$ using $\bar{y}'_i = (x'_{i+_n} - x'_i)/\tau$ as

$$\hat{\sigma}_{y,\text{TOTAL}}^2(\tau) = \frac{1}{2\tau^2(N-2)} \sum_{i=2}^{N-1} (x'_{i-n} - 2x'_i + x'_{i+n})^2 \tag{29}$$

For a detailed description of $\sigma_{y,\text{TOTAL}}^2(\tau)$ see Refs. 21–23.

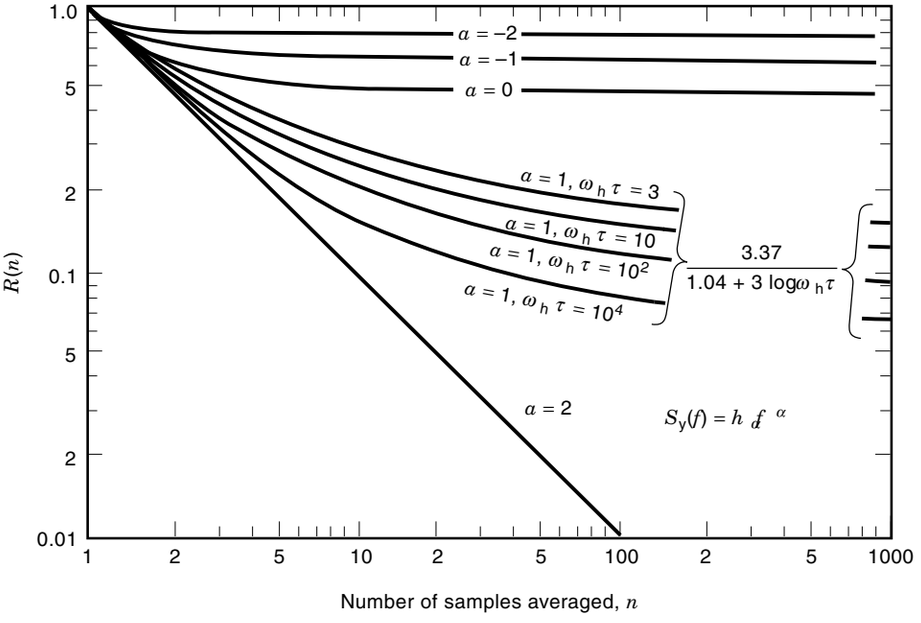

Figure 9. Ratio of the modified Allan variance to the Allan variance, $R(n) = [\text{Mod } \sigma_y^2(\tau)]/\sigma_y^2(\tau)$, as a function of n (15). $\tau = n\tau_0$.

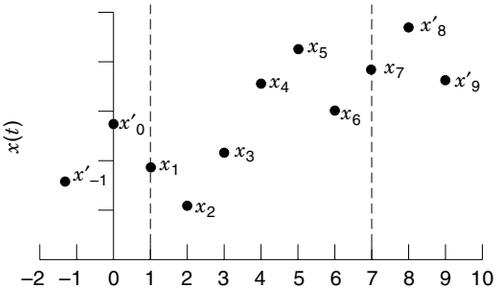

Figure 10. Extension of $\{x_i\}$ for $\sigma_y^2(\tau)$.

CONVERSION BETWEEN TIME-DOMAIN MEASURES AND FREQUENCY-DOMAIN MEASURES

Frequency-domain data $S_\phi(f)$ can be converted to time-domain data $\sigma_y^2(\tau)$ using the relation (1,24)

$$\sigma_y^2(\tau) = \frac{2}{(\pi \nu_0 \tau)^2} \int_0^{f_h} S_\phi(f)\, \sin^4(\pi f \tau)\, df \tag{30}$$

Equation (30) is derived by expressing both $S_\phi(f)$ and $\sigma_y^2(\tau)$ in terms of the autocorrelation function $\mathcal{R}_\phi(\tau)$ of the random process $\phi(t)$ and then combining the two expressions to cancel $\mathcal{R}_\phi(\tau)$ (13). Similarly,

$$\sigma_y^2(\tau) = \frac{2}{(\pi \tau)^2} \int_0^{f_h} S_y(f) \frac{\sin^4(\pi f \tau)}{f^2}\, df \tag{31}$$

Expressions for Mod $\sigma_y^2(\tau)$ (15,24), obtained using a similar procedure, are

$$\text{Mod } \sigma_y^2(\tau) = \frac{2}{n^4(\pi \nu_0 \tau_0)^2} \int_0^{f_h} \frac{S_\phi(f)\, \sin^6(\pi \tau f)}{\sin^2(\pi \tau_0 f)}\, df \tag{32}$$

$$\text{Mod } \sigma_y^2(\tau) = \frac{2}{n^4(\pi \tau_0)^2} \int_0^{f_h} \frac{S_y(f)\, \sin^6(\pi \tau f)}{f^2 \sin^2(\pi \tau_0 f)}\, df \tag{33}$$

The inclusion of f_h as the upper limit of the integral assumes that the term inside the integral is multiplied or "filtered" by an infinitely sharp low-pass filter with cutoff frequency f_h. Table 1 shows the results of Eqs. (31) and (33) for the five types of noise for $2\pi f_h \tau \gg 1$ (1,14–16,24). The results will depend on the type of filter assumed. While an infinitely sharp filter was assumed in Eqs. (30)–(33), actual measurement systems have different filter response.

Table 1. Conversion Factors for $\sigma_y^2(f)$ and Mod $\sigma_y^2(f)$ (1, 14–16, 24)

Noise Type	$S_y(f)$	$\sigma_y^2(f)$	Mod $\sigma_y^2(f)$
Random walk frequency	$h_{-2}f^{-2}$	$(2\pi^2\tau/3)h_{-2}$	$5.42h_{-2}\tau$
Flicker frequency	$h_{-1}f^{-1}$	$(2 \ln 2)h_{-1}$	$0.936h_{-1}$
White frequency	$h_0 f^0$	$h_0/2\tau$	$h_0/4\tau$
Flicker phase	$h_1 f^1$	$\frac{1.038 + 3\ln(\omega_h \tau)}{4\pi^2} h_1 \frac{1}{\tau^2}$	$\frac{3.37}{4\pi^2} h_1 \frac{1}{\tau^2}$
White phase	$h_2 f^2$	$\frac{3f_h}{4\pi^2} h_2 \frac{1}{\tau^2}$	$\frac{3f_h}{4\pi^2} h_2 \frac{1}{n\tau^2}$

Table 2. Empirical Equations for the Number of Degrees of Freedom When Computing Confidence Intervals for the Overlapped Allan Variance (16)

Noise Type	α	No. of Degrees of Freedom
White phase	−2	$\frac{(N+1)(N-2n)}{2(N-n)}$
Flicker phase	−1	$\exp\left[\ln\left(\frac{N-1}{2n}\right)\ln\left(\frac{(2n+1)(N-1)}{4}\right)\right]^{1/2}$
White frequency	0	$\left(\frac{3(N-1)}{2n} - \frac{2(N-2)}{N}\right)\frac{4n^2}{4n^2+5}$
Flicker frequency	+1	$\frac{2(N-2)^2}{2.3N-4.9}$ for $n = 1$
		$\frac{5N^2}{4n(N+3n)}$ for $n \geq 2$
Random-walk frequency	+2	$\frac{N-2}{n}\frac{(N-1)^2 - 3n(N-1) + 4n^2}{(N-3)^2}$

Expressions have also been derived for a single-pole filter (15,25,26). These expressions, along with those in Table 1, constitute the boundaries for $\sigma_y^2(\tau)$ and Mod $\sigma_y^2(\tau)$, given a specific PSD of phase fluctuations (15). For this reason it is important to specify the filter frequency response, including the high cutoff frequency, when specifying the Allan and modified Allan variances of a source.

Generally, conversion from $\sigma_y^2(\tau)$ or Mod $\sigma_y^2(\tau)$ to the frequency domain is not possible, unless specific information about the noise characteristics is known. Greenhall demonstrated that several different spectral densities of random processes can have the same Allan variance (27). However, in the case where the spectral density follows the noise model in Eqs. (13)–(14), a one-to-one correspondence between $S_\phi(f)$ and $\sigma_y^2(\tau)$ and Mod $\sigma_y^2(\tau)$ is found, except that for white PM and flicker PM noise $\sigma_y^2(\tau)$ exhibits the same slope, corresponding to τ^{-2}. Often, uniqueness fails more generally. Some sources have internal phase-locked loops, and their noise spectra deviates from the model in Eqs. (13)–(14) (28); others exhibit 60 Hz and other peaks that will affect $\sigma_y^2(\tau)$ (16,29). Generally, multivariance analysis should be used to obtain frequency-domain coefficients for each type of noise from time-domain data (30).

CONFIDENCE INTERVALS FOR $\sigma_y^2(\tau)$ AND Mod $\sigma_y^2(\tau)$

The Allan variance is defined as the first difference of average fractional frequencies, averaged over an infinite time. Since only a finite number M of frequency samples can be taken, we can only estimate the Allan variance and deviation, and the confidence of this estimate depends on the number of samples.

A simple method to obtain confidence intervals is to use the chi-squared distribution function. The Allan variance has a chi-squared distribution function given by

$$\chi^2 = \text{df}\frac{\hat{\sigma}_y^2(\tau)}{\sigma_y^2(\tau)} \tag{34}$$

where df is the number of degrees of freedom (16). The Allan variance is the sum of the squares of the first differences of adjacent fractional frequency values. If all the first-difference values were independent, then the number of degrees of freedom would be equal to the number of first difference values. This is not the case, and thus other procedures have been used to compute the number of degrees of freedom for $\sigma_y^2(\tau)$ (16). Table 2 shows analytical (empirical) equations that ap-

Table 3. Confidence Intervals for the Nonoverlapped and Fully Overlapped $\sigma_y(\tau)$ (16) and for the Fully Overlapped Mod $\sigma_y(\tau)$ (31–33)[a]

		Confidence Interval (%)					
		Nonoverlapped $\sigma_y(\tau)$		Fullyoverlapped $\sigma_y(\tau)$		Fullyoverlapped Mod $\sigma_y(\tau)$	
n	Noise Type	−	+	−	+	−	+
2	White PM	4.1	4.8	2.9	3.2	3.1	3.4
8		7.7	10.1	2.9	3.2	5.2	6.1
32		13.6	23.1	3.0	3.4	9.7	14
2	Flicker PM	3.7	4.3	2.9	3.1	3.0	3.3
8		7.1	9.0	3.6	4.0	5.7	6.8
32		12.7	20.7	5.2	6.1	11	16
2	White FM	3.6	4.0	2.8	3.0	3.0	3.2
8		6.8	8.6	4.8	5.6	5.8	7.0
32		12.5	20.1	8.8	12	11	16
2	Flicker FM	3.2	3.5	2.6	3.0	2.9	3.2
8		6.1	7.4	5.1	6.0	5.8	7.1
32		11.1	16.8	9.9	14	11	16
2	Random-walk FM	3.0	3.3	3.0	3.3	3.2	3.5
8		5.7	6.8	5.7	7.0	6.4	8.0
32		10.4	15.2	11	16	12	19

[a] Confidence intervals for the nonoverlapped $\sigma_y(\tau)$ were obtained using df in Table 2 (16). The degrees of freedom used for the fully overlapped $\sigma_y(\tau)$ were computed using numerical methods and are approximately equal to those obtained using Table 2 (16, 19). Confidence intervals for the fully overlapped Mod $\sigma_y(\tau)$ were obtained from Ref. 33. $N = 1025$.

proximate the number of degrees of freedom for the fully overlapped Allan variance (16). The equation depends on the noise type. For nonoverlapped estimates, n in Table 2 is equal to 1, and N refers to the *equivalent* number of time samples for $\tau = n\tau_0$ given by Int$((N - 1)/n) + 1$, where Int( ) refers to the integer part.

Usually a $(p \times 100)$ % confidence interval is computed, where p is the probability that the true Allan variance or Allan deviation is within the computed confidence interval. The $(p \times 100)$ % confidence interval for the overlapped Allan variance is given by

$$\chi^2\left(\frac{1-p}{2}\right) < \mathrm{df}\,\frac{\hat{\sigma}_y^2(\tau)}{\sigma_y^2(\tau)} < \chi^2\left(p + \frac{1-p}{2}\right) \tag{35}$$

$$\frac{df}{\chi^2\left(p + \frac{1-p}{2}\right)}\hat{\sigma}_y^2(\tau) < \sigma_y^2(\tau) < \frac{df}{\chi^2\left(\frac{1-p}{2}\right)}\hat{\sigma}_y^2(\tau) \tag{36}$$

where the chi-squared value $\chi^2(C)$ for $(p \times 100)$ % confidence can be obtained from chi-squared distribution tables or from several computer programs. The $(p \times 100)$ % confidence interval for the Allan deviation is

$$\sqrt{\frac{df}{\chi^2\left(p + \frac{1-p}{2}\right)}}\,\hat{\sigma}_y(\tau) < \sigma_y(\tau) < \sqrt{\frac{df}{\chi^2\left(\frac{1-p}{2}\right)}}\,\hat{\sigma}_y(\tau) \tag{37}$$

The chi-squared distribution can also be used to find the confidence intervals for Mod $\sigma_y^2(\tau)$.

Walter (31) and Greenhall (32) have derived expressions for the number of degrees of freedom of Mod $\sigma_y^2(\tau)$ using different procedures. These expressions are complicated and will not be presented here. The two methods yield similar results (33). Table 3 shows the confidence intervals for $\sigma_y(\tau)$ with no overlap and full overlap (16,19), and for Mod $\sigma_y(\tau)$ (31–33) for the five noise types. In general, the confidence intervals for the fully overlapped $\sigma_y(\tau)$ are smaller than those for the nonoverlapped $\sigma_y(\tau)$. For random-walk FM noise, the confidence intervals for the nonoverlapped and the fully overlapped $\sigma_y(\tau)$ are approximately the same, although Table 3 shows a small degradation when using fully overlapped estimates. This degradation is due to the approximations used in the analytical expressions. Table 3 also shows that the confidence intervals for the fully overlapped Allan deviation are smaller than the ones for the fully overlapped modified Allan deviation. Nevertheless, the modified deviation is generally smaller than the Allan deviation, and thus the absolute confidence intervals for the two are similar.

BIBLIOGRAPHY

1. E. S. Ferre-Pikal et al., Draft revision of IEEE Std 1139-1988: Standard definitions of physical quantities for fundamental frequency and time metrology—random instabilities, *Proc. 1997 IEEE Int. Freq. Control Symp.,* 1997, pp. 338–357.
2. R. L. Sydnor and D. W. Allan (eds.), *Handbook Selection and Use of Precise Frequency and Time Systems,* International Telecommunication Union, Geneva, Switzerland, 1997.
3. International Radio Consultative Committee (CCIR), Report 580, *Characterization of Frequency and Phase Noise,* 1986, pp. 142–150.
4. H. Hellwig, *Frequency Standards and Clocks: A Tutorial Introduction,* Technical Note 616, Washington, DC: U.S. National Bureau of Standards, 1977.
5. J. R. Vig and F. L. Walls, Fundamental limits on the frequency stabilities of crystal oscillators, *IEEE Trans. Ultrason. Ferroelectr. Freq. Control,* **42**: 576–589, 1995.

6. *IEEE Guide for Measurements of Environmental Sensitivities of Standard Frequency Generators,* IEEE Std. 1193, Piscataway, NJ: IEEE Press, 1994.
7. W. D. Lee et al., The accuracy evaluation of NIST-7, *IEEE Trans. Instrum. Meas.,* **44**: 120–124, 1995. An example of evaluating the uncertainties of an atomic frequency standard.
8. B. N. Taylor and C. E. Kuyatt, *Guidelines for Evaluating and Expressing the Uncertainty of NIST Measurement Results,* Technical Note 1297, Washington, DC: National Institute of Standards and Technology, 1994.
9. F. L. Walls, The influence of pressure and humidity on the medium and long-term frequency stability of quartz oscillators, *Proc. 42nd Annu. Symp. Freq. Control,* Baltimore, MD: 1988, IEEE Catalog No. 88CH2588-2, pp. 279–283.
10. J. J. Gagnepain, Sensitivity of quartz oscillators to the environment: Characterization methods and pitfalls, *IEEE Trans. Ultrason. Ferroelectr. Freq. Control,* **37**: 354, 1990.
11. F. L. Walls and J. J. Gagnepain, Environmental sensitivities of quartz oscillators, *IEEE Trans. Ultrason. Ferrelectr. Freq. Control,* **39**: 241–249, 1992.
12. J. R. Vig and T.R. Meeker, The aging of bulk acoustic wave resonators, filters and oscillators, *Proc. 45th Annu. Symp. Freq. Control,* Los Angeles, CA: 1991, IEEE, Catalog No. 91CH2965-2, pp. 77–101.
13. J. A. Barnes et al., Characterization of frequency stability, *IEEE Trans. Instrum. Meas.,* **IM-20**: 105–120, 1971.
14. D. W. Allan et al., Standard terminology for fundamental frequency and time metrology, *Proc. 42nd Annu. Symp. on Freq. Control,* Baltimore, MD: 1988, IEEE Catalog No. 88CH2588-2, pp. 419–425.
15. D.B. Sullivan et al., *Characterization of Clocks and Oscillators,* Technical Note 1337, National Institute of Standards and Technology, 1990.
16. D. A. Howe, D.W. Allan, and J. A. Barnes, Properties of signal sources and measurement methods, *Proc. 35th Annu. Symp. Freq. Control,* Electronic Industries Association 1981, Washington, DC, Philadelphia, PA: 1981, pp. A1–A47; also in Ref. 4.
17. T. E. Parker, Characteristics and sources of phase noise in stable oscillators, *Proc. 41st Annu. Symp. Freq. Control,* Philadelphia, PA: 1987, IEEE Catalog No. 87CH2427-3, pp. 99–110.
18. L. M. Nelson, C. W. Nelson, and F. L. Walls, Relationship of AM nose to PM noise in selected RF oscillators, *IEEE Trans. Ultrason. Ferroelectr. Freq. Control,* **41**: 680–684, 1994.

18a. F. L. Walls, Correlation between upper and lower noise sidebands, to be published in *Proc. 1998 IEEE Int. Freq. Control Symp.,* Pasadena, CA, May 1998.

19. S. R. Stein, Frequency and time—their measurement and characterization, in E. A. Gerber and A. Ballato (eds.), *Precision Frequency Control,* New York: Academic Press, 1985, vol. 2, chap. 12.
20. D. W. Allan and J. A. Barnes, Modified Allan variance with increased oscillator characterization ability, *Proc. 35th Annu. Symp. Freq. Control,* Electronic Industries Assoc. 1981, Philadelphia, PA: 1981, pp. 470–474.
21. D. A. Howe, An extension of the Allan variance with increased confidence at long-term, *Proc. 1995 IEEE Int. Freq. Control Symp.,* San Francisco, CA: 1995, IEEE Catalog No. 95CH35752, pp. 321–329.
22. D. A. Howe, Methods of improving the estimation of long-term frequency variance, *Proc. European Frequency and Time Forum,* Swiss Foundation for Research in Microtechnology, Neuchatel, Switzerland: 1997, pp. 91–99.
23. D. A. Howe and C. A. Greenhall, Total variance: A progress report on a new frequency stability characterization, *Proc. 29th Ann. Precise Time Time Interval PTTI Syst. Appl. Meet.,* Long Beach, CA: 1997, pp. 39–48.
24. F. L. Walls et al., Time-domain frequency stability calculated from the frequency domain: An update, *Proc. 4th Eur. Frequency Time Forum,* Swiss Foundation for Research in Microtechnology, Neuchatel, Switzerland: 1990, pp. 197–204.
25. P. Lesage and C. Audoin, Characterization and measurement of time and frequency stability, *Radio Sci.,* **14** (4): 521–539, 1979.
26. P. Lesage and T. Ayi, Characterization of frequency stability: Analysis of the modified Allan variance and properties of its estimate, *IEEE Trans. Instrum. Meas.,* **IM-33**: 332–336, 1984.
27. C. A. Greenhall, Does the Allan variance determine the spectrum?, *Proc. 1997 IEEE Inter. Freq. Control Symp.,* Orlando, FL: 1997, IEEE Catalog No. 97CH36016, pp. 358–365.
28. F. L. Walls and S. R. Stein, *Servo techniques in oscillators and measurement systems,* Technical Note 692, Washington, DC: U.S. National Bureau of Standards, pp. 1–20, 1976.
29. J. Rutman and F. L. Walls, Characterization of frequency stability in precision frequency sources, *Proc. IEEE,* **79**: 952–960, 1991.
30. F. Vernotte et al., Oscillator noise analysis: multivariance measurement, *IEEE Trans. Instrum. Meas.,* **IM-42**: 342–350, 1993.
31. T. Walter, Characterizing frequency stability: A continuous power-law model with discrete sampling, *IEEE Trans. Instrum. Meas.,* **IM-43**: 69–79, Feb. 1994.
32. C. A. Greenhall, Estimating the modified Allan variance, *Proc. 1995 IEEE Int. Freq. Control Symp.,* San Francisco, CA: 1995, IEEE Catalog No. 95CH35752, pp. 346–353.
33. M. A. Weiss et al., Confidence on the modified Allan variance, *Proc. 9th Eur. Frequency Time Forum,* Besançon, France, 1995, pp. 153–165.

EVA S. FERRE-PIKAL
FRED L. WALLS
National Institute of Standards and Technology